AMS 2024 Annual Meeting 28 January – 1 February, 2024

V7

The Retrieval of Surface Pressure and Wind Speed over Ocean using NOAA-20 ATMS Measurements through a U-Net Machine Learning Algorithm

Zichao Liang[1], Yong-Keun Lee[2], Christopher Grassotti[2], Lin Lin[3], and Quanhua (Mark) Liu[3]

1. University of Maryland, Department of Computer Science, 2. University of Maryland, Cooperative Institute for Satellite Earth System Studies and NOAA/NESDIS/STAR (yong-keun.lee@noaa.gov) 3. NOAA/NESDIS/STAR

Abstract

A U-Net algorithm was used to retrieve surface pressure and wind speed over the ocean within tropical cyclones (TCs) and their neighboring areas using NOAA-20 Advanced Technology Microwave Sounder (ATMS) reprocessed Sensor Data Record (SDR) brightness temperatures (TBs) and geolocation information. For TC locations, International Best Track Archive for Climate Stewardship (IBTrACS) data have been used over the North Atlantic Ocean and West Pacific Ocean between 2018 and 2021. The European Center for Medium-Range Weather Forecasts (ECMWF) Reanalysis v5 (ERA5) surface pressure and wind speed were employed as reference labels. Preliminary results demonstrated that the visualizations for wind speed and pressure matched the prediction and ERA5 location. The residual biases and standard deviations between the predicted and reference labels were about 0.15 m/s and 1.95 m/s, respectively, for wind speed and 0.48 hPa and 2.67 hPa, respectively, for surface pressure, after applying cloud screening for each ATMS pixel. This indicates that the U-Net model is effective for surface wind speed and surface pressure estimates over general ocean conditions.

Data and Methods

- NOAA-20 ATMS: brightness temperature (22 microwave channel reprocessed Sensor Data Record (SDR)), latitude, longitude, satellite zenith angle during 2018-2021.
- The European Centre for Medium-Range Weather Forecasts (ECMWF) Reanalysis v5 (ERA5) during 2018-2021. Temporal: 1 hour interval, Spatial: quarter degree in latitude and longitude
- The International Best Track Archive for Climate Stewardship (IBTrACS): during 2018-2021 over the Northwestern Pacific, North Atlantic ocean.
- For each TC location in IBTrACS, the closest NOAA-20 ATMS FOV is selected within +/- 3 hours and within the distance of 200 km. Once the closest ATMS location is determined, 47 scan lines observed after the location and 48 scan lines observed before the location are combined to generate 96 scan lines (corresponding to 8 ATMS granules)
- NOAA-20 ATMS data 12 (scan lines for each granule) x 96 (FOVs) x 25 (variables)
25 variables includes 22 channel reprocessed BTs (SDR), latitude, longitude, and satellite zenith angle.
- Reference data from ERA5 include surface pressure and surface wind speed
- Surface wind speed is calculated by the square root of the sum of squares of u and v wind speed.
- The output includes 2 variables (surface pressure and surface wind speed) for each FOV.
- U-Net: the evolution of the traditional convolutional neural network (CNN) algorithm

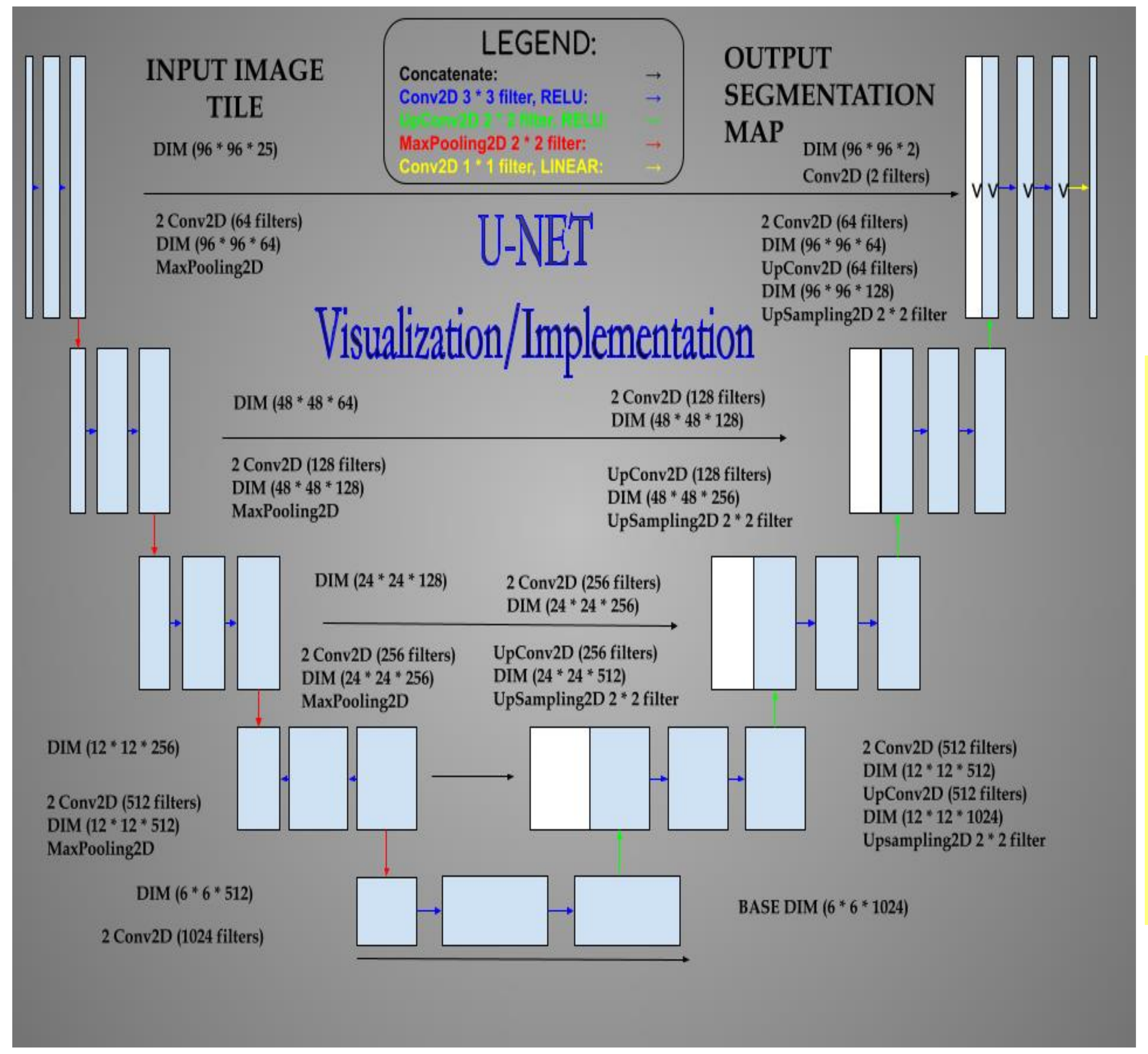

Figure 1. U-Net architecture in this study. The U-Net follows a symmetric U shape divided into two paths leading down and up the network, called the contracting path and the expansive path: a contracting path (i.e., encoder), spatial filtering layers, pooling layers, a corresponding expansive path (i.e., decoder)

Flowchart of the data preprocessing

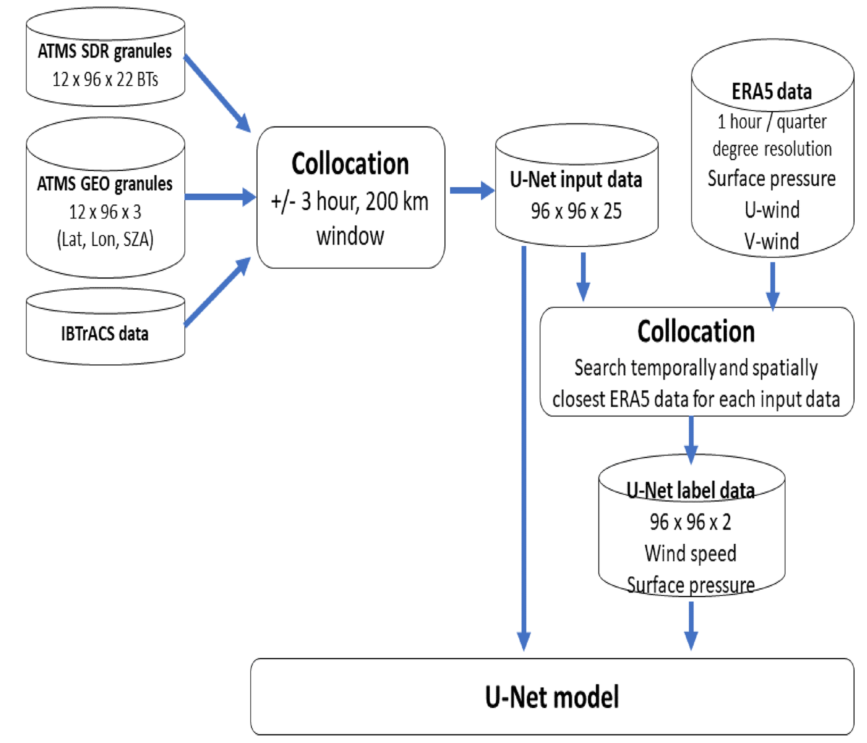

Figure 2. NOAA-20 ATMS SDR brightness temperature (22 channels), latitude, longitude, satellite zenith angle, IBTrACS data and ERA5 surface pressure and surface wind speed with 1 hour temporal resolution and quarter degree spatial resolution in latitude and longitude. For each TC location in IBTrACS, ATMS data are selected and be combined to have 96 (scan lines) x 96 (FOVs) x 25 (variables, BTs, lat, lon, sza) in one file. Total 266 files of ATMS data have been generated (only for pure ocean). 239 files have been used for the training and 27 files for the independent validation.

Learning Rate Base	Learning Rate Decay	Batch Size	Epochs	Activation Function	Cost Function	Regularization	Learning Rate Schedule
0.0001	0.99	16	500	ReLU/Linear	MSE	None	Exponential Decay

Table 1. Most key hyperparameter settings

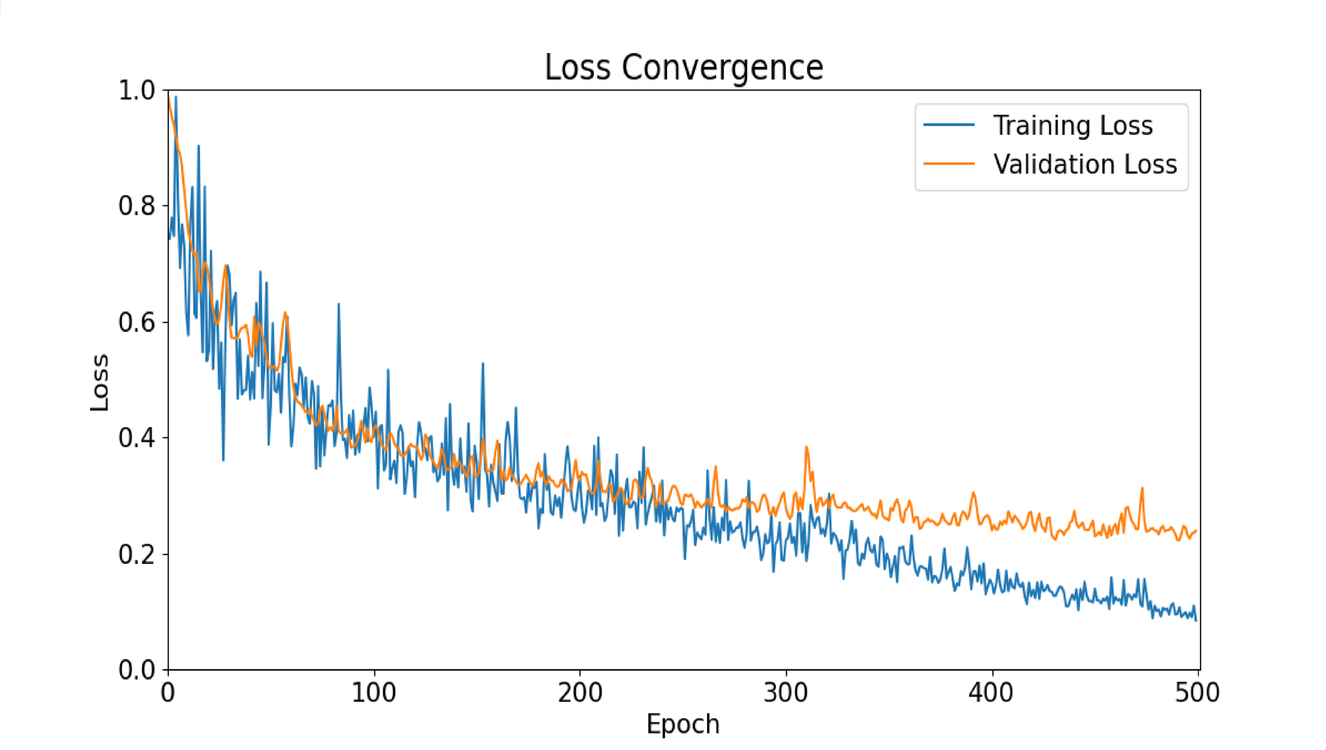

Figure 3. Loss convergence for U-Net training (239 tiles) and validation (27 tiles). Both the training and validation losses converged significantly faster in the beginning epochs and the rate of convergence slowed towards the latter epochs. After 220 epochs, the difference between the training and validation losses seemed to gradually increase, showing potential overfit.

Residual Statistics (U-Net Pred-ERA5 Label)	Without Clearance of CLW Pixels > 0.3 mm		With Clearance of CLW Pixels > 0.3 mm	
	WS (m/s)	Surface Pressure (hPa)	WS (m/s)	Surface Pressure (hPa)
Bias	0.125	0.563	0.133	0.481
Standard Deviation	2.125	2.845	1.947	2.674
Minimum	−19.92	−13.91	−12.83	−13.91
Maximum	19.60	39.41	18.19	26.43
Correlation Coefficient	0.812	0.864	0.791	0.837
# Samples	27 tiles			
Prediction Loss/Accuracy	MSE (Loss): 0.2632; MAE: 0.3791			

Table 2. Mean squared error, mean absolute error and residual statistics (U-Net prediction – ERA5) surface pressure and surface wind speed with/without clearance of cloud liquid water pixels (CLW > 0.3 mm).

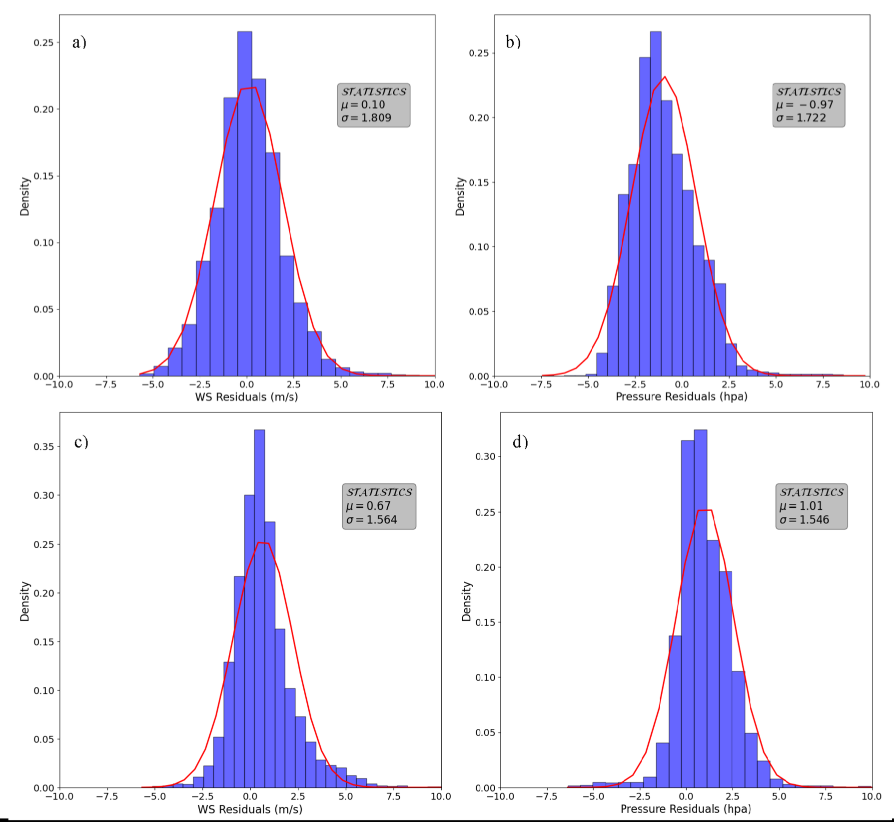

Figure 4. Single sample residual histograms (U-Net prediction—ERA5) for (**a**,**b**) surface wind speed and surface pressure residuals, respectively, for sample valid on 10 October 2018 at 06 UTC, while (**c**,**d**) contain similar residuals but for the sample valid on 14 September 2018 at 06 UTC.

Predicted and ERA5 surface wind speed

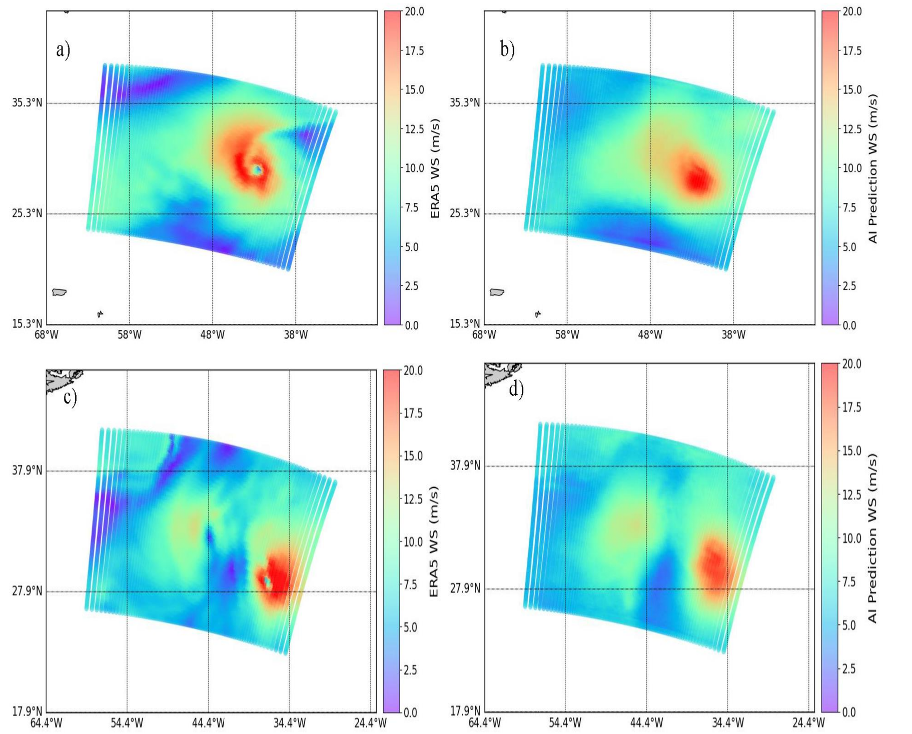

Figure 5. U-Net prediction and ERA5 surface wind speed maps. (**a**,**b**) represent ERA5 and U-Net predicted wind speed, respectively, of sample valid on 10 October 2018 at 06 UTC (Leslie), while (**c**,**d**) represent ERA5 and U-Net predicted wind speed, respectively, of sample valid on 14 September 2018 at 06 UTC (Joyce in the middle and Helene on the right-side).

Predicted and ERA5 surface pressure

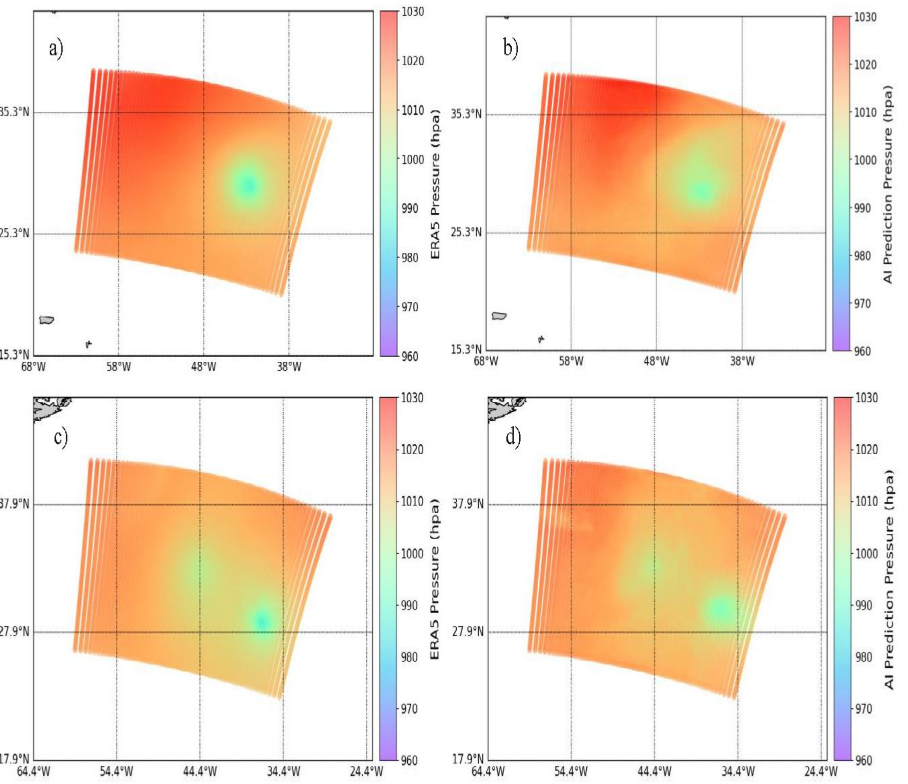

Figure 6. U-Net prediction and ERA5 surface pressure maps. (**a**,**b**) represent ERA5 and U-Net predicted wind speed, respectively, of sample valid on 10 October 2018 at 06 UTC (Leslie), while (**c**,**d**) represent ERA5 and U-Net predicted surface pressure, respectively, of sample valid on 14 September 2018 at 06 UTC (Joyce in the middle and Helene on the right)

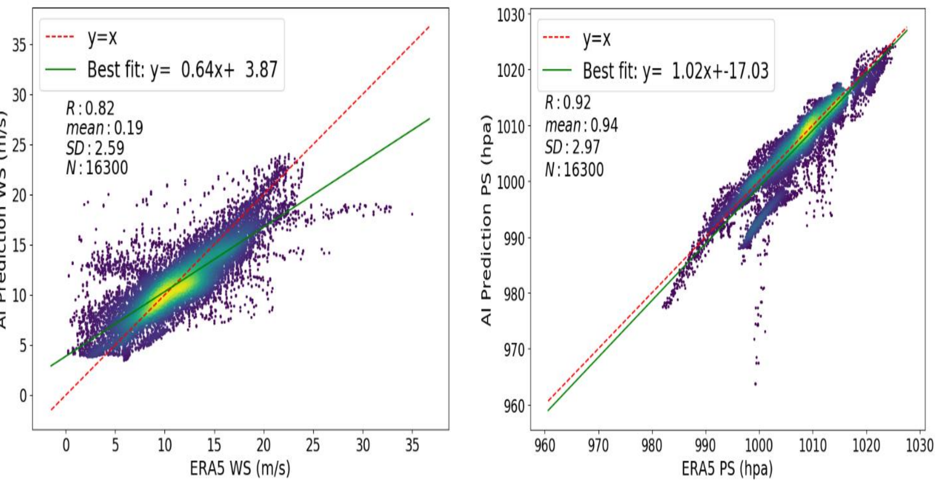

Figure 7. Scatterplots of U-Net prediction vs. ERA5 for (**a**) wind speed (m/s) and (**b**) surface pressure (hPa) across all 27 test samples. The pixels included in this analysis were selected from within a 350 km radius circle centered on the TC. The data distribution changes from dense to sparse as the color shifts from yellow to blue. (R: Pearson correlation coefficients; SD: standard deviation; N: number of selected pixels).

Total: 27 Samples	Bias (PRED-IBTrACS)	Std. (PRED-IBTrACS)	RMSE
Sfcp (hpa)	13.1929	17.2667	21.7300
WS (m/s)	−12.3989	10.4160	16.5794

Table 3. Statistics of the estimates of maximum sustained surface wind speed and minimum surface pressure of 27 tropical cyclone cases compared to IBTrACS.

Summary

A modified U-Net algorithm was employed to estimate surface wind speed and surface pressure surrounding the TC areas. ATMS data and collocated ERA5 were chosen based on the time and location of TCs in the IBTrACS database for the period 2018 to 2021, located in the Northwest Pacific and North Atlantic basins.
The U-Net prediction showed promising results. The residual biases and standard deviations between the U-Net predicted and ERA5 reference labels were about 0.13 m/s and 1.95 m/s for wind speed and 0.48 hPa and 2.67 hPa for surface pressure, respectively, after cloud screening for each ATMS pixel. This indicates that the U-Net model is effective for near-TC wind speed and pressure estimates for more general over-ocean conditions.

References

Liang, Z.; Lee, Y.-K.; Grassotti, C.; Lin, L.; Liu, Q. MachineLearning-Based Estimation of Tropical Cyclone Intensity from Advanced Technology Microwave Sounder Using a U-Net Algorithm. Remote Sens. **2024**, 16, 77. https://doi.org/10.3390/rs16010077

Acknowledgement and Disclaimer

This work is supported by NOAA under Grant NA19NES4320002 to the Cooperative Institute for Satellite and Earth System Studies (CISESS) at the University of Maryland/Earth System Science Interdisciplinary Center (ESSIC). The views, opinions, and findings contained in this presentation are those of the authors and should not be construed as an official NOAA or U.S. Government position, policy, or decision.